Anais XIII Simpósio Brasileiro de Sensoriamento Remoto, Florianópolis, Brasil, 21-26 abril 2007, INPE, p. 6519-6526.

Spectral Mixture Analysis of EO-1 Hyperion Imagery focused on the Spatial-Temporal Variability of the Amazon Floodplain Multicomponental Waters

Conrado de Moraes Rudorff [1]
Evlyn Márcia Leão de Moraes Novo [1]
Lênio Soares Galvão [1]

[1] Instituto Nacional de Pesquisas Espaciais - INPE
Caixa Postal 515 - 12245-970 - São José dos Campos - SP, Brasil
{cmr, evlyn, lenio}@ltid.inpe.br

Abstract. The Amazon floodplain water composition undergoes intensive variations along the year as a response to the annual flood pulse. The present study analyzes the spectral mixtures of the optically active substances (OAS) in the Amazon floodplain waters with spaceborne hyperspectral images. The test site was located upstream the confluence of Amazon (white water) and Tapajós (clear-water) rivers, where two Earth Observing One (EO-1) Hyperion images were acquired. The first image was acquired on September 16, 2001, during the falling water period of the Amazon River. The second image was acquired on June 23, 2005, at the end of the high water period. The images were pre-processed to remove stripes of anomalous pixels and were converted from radiance to surface reflectance values, thus, correcting the effects of atmospheric absorption and scattering. A sequential procedure with the techniques Minimum Noise Fraction (MNF), Pixel Purity Index (PPI) and n-dimensional visualization of the MNF feature space was employed, within the spectral range of 457-885 nm, to select end-members from both images. A single set of end-members was gathered to represent the following spectrally unique water constituents: clear-water; dissolved organic matter; suspended sediments; and phytoplankton. The Linear Spectral Unmixing (LSU) algorithm was applied to each Hyperion image in order to map the spatial distribution of these constituents, in terms of sub-pixel fractional abundances. The variability in the concentration of suspended inorganic matter (SIM) and phytoplankton between high and falling flood periods was accessed and discussed.

Keywords: Amazon; floodplains, water quality, remote sensing, hyperspectral imagery, spectral mixture analysis.

1. Introduction

Natural waters are complex physical-chemical-biological media comprising living, non-living, and once-living materials that may be present in aqueous solution or suspension. The materials that interact with the light field in water column are referred to as Optically Active Substances (OAS). The main OAS in natural inland water are: phytoplankton; dissolved organic matter (DOM); and suspended inorganic matter (SIM). The optical properties of these substances are closely related to the water quality, and have been discussed in detail by several authors (e.g., Bukata, 2000; Dekker, 1993; Kirk, 1994). Pure water molecules itself, with heterogeneities resulting from small-scale water eddies, also contributes to determine the bulk optical properties of natural water bodies (Bukata, 2000).

Water and its constituents shape the biodiversity and aquatic ecosystem productivity in the Amazon region (Junk, 1997). The significant spatial-temporal variability in the constitution of Amazon floodplain water is derived from the ever-changing water level over a vast and diverse environment, which makes the assessment of water quality extremely challenging. Remote sensing methods and technology have been largely considered and tested for this assessment, but so far water color sensors (e.g., SeaWiFS and MODIS) have not been suitable for mapping inland waters due to spatial resolution constraints, and other land sensors (e.g., Landsat-7/ETM$^+$ and CBERS-2/CCD) due to radiometric and spectral limitations.

Hyperion is a hyperspectral imaging sensor that was launched in November 2000, on board of the Earth Observing One (EO-1) satellite. The key feature of Hyperion imagery is that it provides access to a measurement of a near complete spectrum, from visible (VIS) to

short wave infrared (SWIR) range, for each pixel using narrow wavebands (10 nm). Hyperspectral imagery presents a number of opportunities for interpretation and analysis (Aspinall et al., 2002). Spectral mixture analysis methods have been widely used to determine sub-pixel composition by modeling the abundances of spectrally unique materials, which are commonly referred to as spectral end-members (Adams et al., 1986). However, the success of this approach depends on the representation and availability of 'pure' end-members. Preferably, the end-members should be obtained directly from the image under analysis (Kruse et al., 2003), once the reflectance spectra measured in laboratory do not account for undesirable environmental and instrumental signal variations which are measured by an orbital sensor. Novo and Shimabukuro (1994) pointed out the exertion of finding pure end-members to represent each individual OAS in water.

The major objective of the present study is to evaluate the use of Hyperion images to map water constituents in the Amazon floodplain, by determining the fractional abundances of clear-water, DOM, SIM and phytoplankton, using a Linear Spectral Unmixing (LSU) algorithm.

2. The Linear Spectral Unmixing Algorithm

The main concept of spectral mixture analysis to study the water composition is that the reflectance measured at a given pixel is represented by the sum of end-members, which represent each OAS, weighted by its relative proportion or abundance (Novo and Shimabukuro, 1994)

$$R_{pi} = \sum f_j r_{ij} + \varepsilon_i \qquad (1)$$

where, for a given pixel p, R_{pi} is the water remote sensing reflectance of the i^{th} band, j represents the end-member for a certain OAS, f_j is the fractional abundance of the j^{th} end-member, r_{ij} is the j^{th} end-member reflectance of the i^{th} band, and ε_i is the error in the i^{th} waveband. The inversion process of (1) determines the fractional abundance of each end-member.

3. Site Location and Description

The experimental site is situated just upstream the confluence of Amazon and Tapajós rivers in Pará State, Brazil (**Figure 1**). The collection of water bodies in this floodplain region lies on sandy deposits of Quaternary sediments. An annual flood pulse propagating along the Amazon Basin characterizes a monomodal hydrologic regime (Junk, 1997), which can be summarized, in terms of the water level of the floodplain-river system, into four important periods: low; rising; high; and falling. Significant seasonal changes in the water quality respond to this forcing function of the flood pulse. At the beginning of rising water level period submerged organic material, such as once-living plants and animals, begins to decompose, and the development of a great amount of macrophytes takes place near the margins of water bodies. During high water level period, suspended matter with associated nutrients are introduced from the Amazon River to the floodplain lakes and deposit over regions with reduced turbulence. Macrophyte continues to grow, once they are very efficient in retrieving the nutrients available in the water. This causes the nutrients to be less available for phytoplankton. In fact, the major events of phytoplankton blooms occur when macrophytes begin to decompose at the falling water level period. Also, during this period some environmental factors favor the re-suspension of sediments and nutrients deposited at the bottom of the lakes, which along with intense solar illumination induce the development of phytoplankton blooms (Junk, 1997).

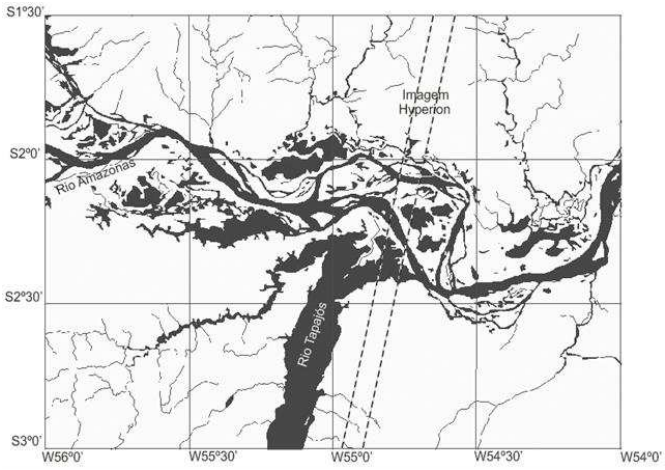

Figure 1 - Location map of the study area. The parallel traced lines present the swaths of the Hyperion images collected over the area.

4. Hyperion data

An archived Hyperion image (EO1H2270622001259111PF), acquired on September 16, 2001, was identified within the USGS EROS Data Center, and showed a wide range of multi-component mixtures along the floodplain waters. In the hydrologic context, this image represented the falling water period. A second Hyperion image (EO1H2270612005174110PV) was programmed and successfully collected over the same site on June 23, 2005, at the end of the high water period.

5. Methods

The Hyperion images were preprocessed according to the following steps: de-striping to remove anomalous pixels (Han et al., 2002); correction of radiance-calibrated data to surface reflectance using Atmospheric CORrection Now (ACORN) model-based software that uses licensed MODTRAN4 technology (AIG, 2001); removal of land targets using a mask established by a threshold of 1% reflectance signal for the 2300 nm band; and spectral range subsetting (457-885nm).

In order to minimizing the reliance on a priori or outside information and derive the maximum information from the hyperspectral reflectance data, a semi-automated procedure was used for the end-member extraction directly from the Hyperion images, as proposed by Kruse et al. (2003). This procedure is implemented in the ENVI image analysis software, and includes: spectral data reduction using the Minimum Noise Fraction (MNF) transformation (Green et al., 1988; Kruse et al., 1993); spatial data reduction using the Pixel Purity Index (PPI) (Kruse et al., 1993); and end-member selection using a n-Dimensional Visualizer (Kruse et al., 1993). Once the end-members were selected they were identified according to their spectral properties. As the two Hyperion images were acquired presenting much different conditions of water quality, it was considered that the set of end-members selected from each image should be combined to form one unique set of end-members to represent clear-water and waters dominated, individually, by each OAS (DOM, SIM, and phytoplankton). This strategy was adopted to increase the availability of 'pure' end-members. At last, the fractional abundances (*f*) of clear-water and the OAS were mapped applying LSU to each Hyperion reflectance image.

6. Results and Discussion

The clear-water and DOM end-members (**Figure 2**) were extracted from June 23, 2005 Hyperion image, and the SIM and phytoplankton end-members (**Figure 2**) were extracted from September 16, 2001 Hyperion image. Clear-water presents very low concentrations of OAS; consequently, the spectral reflectance is low and shaped according to the optical properties of pure water molecules, which produce an exponential increase of absorption towards longer wavelength and scattering towards shorter wavelength, over the VNIR. Dissolved organic matter increases the water absorption exponentially towards shorter wavelengths (Kirk, 1994) and produces fluorescence in the red and NIR bands. The phytoplankton spectrum shows a prominent reflectance peak in the green region, representing the minimal aggregate absorption of all algal pigments. The red band of chlorophyll (Chl) absorbance at 670–675 nm was prominent and sensitive to both pigment absorption and aggregate scattering by algae and other particles. A pronounced absorption feature at about 620–630 nm was present. A second prominent reflectance peak was observed near 700 nm, a wavelength longer than the red absorbance band of algal pigments and lower than the region of maximal water absorbance. Although Chl fluorescence, centered near 685 nm, contributes to this feature, the majority of the radiance measured in this peak is due to scattering from algal cells and other particulate matter (Dekker 1993). When algae blooms occur, the phytoplankton grows more intensively in the upper layer of the water column. In this case, phytoplankton will dominate the surface reflectance signal detected by the remote sensor. However, it is necessary to consider the presence of spectral mixtures, especially from SIM, within the pixel extracted for the phytoplankton end-member. The spectrum of water dominated by SIM is characterized by an increase of reflectance through all the VNIR spectral range, but more particularly towards the 580-680 nm range (Novo et al., 1991).

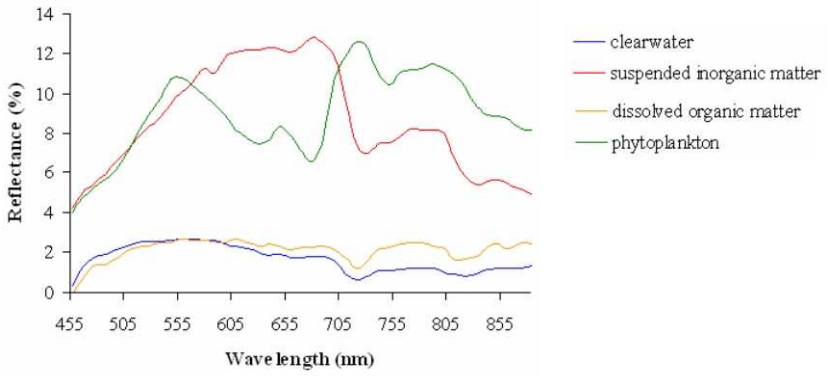

Figure 2 - Hyperion end-members spectra of waters dominated by optically active substances.

Figure 3 presents the results obtained from the application of LSU to both Hyperion images. Negative or over 1 estimates of end-member abundances (f_j) were derived from the assumption of the LSU, which states that the sum of the fractions should be equal to 1; therefore, if the model overestimates one fraction, any of the other fractions may have to be underestimated in order to compensate for the overestimation. Clear-water and DOM abundances mapped by LSU showed reliable results only over non turbid waters, where the LSU determined values of either $f_{\text{clear-water}}$ or f_{DOM} close to 1 and abundance values of the others OAS close to 0. Over non turbid waters, the LSU abundance results for clear-water ($f_{\text{clear-water}}$) and DOM (f_{DOM}) were very sensitive to slight reflectance variation, controlled by: water molecules scattering and DOM absorption, in the blue bands; and water molecules absorption and DOM fluorescence, in the red and NIR bands. However, over turbid waters the spectral influence of SIM and phytoplankton caused total uncertainties on the results of $f_{\text{clear-}}$

$_{water}$ and f_{DOM}. The reflectance of SIM is dominant over all the others OAS in water. Thus, the LSU showed the best potential to estimate the abundance of SIM (f_{SIM}); but at the same time, SIM was the major responsible for introducing uncertainties upon the fractional abundances mapped for the others OAS. This explains the spatial relation observed from the high water image between the RMS error (**Figure 3.f**) and the increase of f_{SIM} (**Figure 3.e**). The falling water RMS error image presented larger uncertainties over lakes with intense mixture of algae and high SIM concentration, as well as in area of muddy shallow lakes. The dominant influence of SIM reflectance, not only detracts the evidences of phytoplankton Chl features over the spectra, but also produces an opposite spectral behavior on the red bands, where Chl acts as an absorber and SIM as a scatterer. This effect led the LSU to map phytoplankton abundance ($f_{phytoplankton}$) with negative values over waters with strong SIM influence.

The low reflectance signal of water is highly affected by undesired radiance fluxes that are captured by the sensor (Bukata, 2000) and introduce uncertainties to the results as well. For instance, the high water RMS error image (**Figure 3.f**) pointed larger uncertainties over regions affected by haze; mainly concentrated at the north of Tapajós River and south of the Amazon River. The presence of haze seemed to affect the values of $f_{phytoplankton}$, causing a fake increase.

Figure 3 - True color composition (RGB: 640; 549; 457nm) of Hyperion image collected on: (a) June 23, 2005; and (g) September 16, 2001. Hyperion fractional end-member abundance results presented as color images: (b) and (h) $f_{clear\text{-}water}$; (c) and (i) f_{DOM}; (d) and (j) $f_{phytoplankton}$; (e) and (l) f_{SIM};. (f) and (m) RMS error.

In order to discuss the meaningfulness of the results, in terms of a tool to be used to explain the temporal variability of water composition, four representative water bodies were selected over the study site: Tapajós River; Amazon River; Lake Aritapera; and Lake Curumu. The reflectance spectra and the end-member abundances of SIM and phytoplankton were analyzed (**Figure 4**).

The Tapajós River is a large tributary of the Amazon. The euphotic zone in the Tapajós is deep, but these clear-waters are poor in nutrients when compared to the Amazon River (Junk, 1997). Over the Tapajós, at both water level periods, the model determined values of $f_{clear\text{-}water}$

close to 1 and fractional abundances of the OAS (f_{DOM}; f_{SIM}; e $f_{phytoplankton}$) close to 0. This was expected since the concentrations of OAS in clear-waters are low. The reflectance spectra and the calculated abundances both evidenced an increase of algae production in the Tapajós River towards the falling water period (**Figure 4**).

The Amazon is the main river of the floodplain. The water reflectance of the Amazon River is permanently dominated by SIM. The model showed good efficiency to map, at both water level periods, f_{SIM} higher than 0.5 and $f_{phytoplankton}$ close to 0 (**Figure 4**). The water of the Amazon River has nitrogen limitations (Junk, 1997), shallow euphotic zone, and turbulence. These factors limit the growth of phytoplankton throughout the seasons. According to Barbosa (2005), the SIM concentration in the Amazon River at the falling water period is around 20 mg l^{-1}. The concentration of SIM measured at the field during high water was 64.33 mg l^{-1}. From these values it is possible to consider a variation of around 40 mg l^{-1} in the concentration of SIM, between the two periods. This resulted in a higher f_{SIM} mapped for high water. The SIM concentration at high water is more than two times higher than at falling water period, but f_{SIM} observed for high (0.66) and falling (0.58) water periods do not demonstrate this same direct proportion. This can be explained by the variation of the inorganic and organic fraction of the total suspended matter composition observed between these periods (Barbosa, 2005), as well as the nonlinear effects between f_{SIM} determined by LSU and the actual SIM concentration (Mertes et al., 1993; Rudorff et al., 2006). In fact, the spectra measured over Amazon water during high water presented higher reflectance values in, practically, the whole spectral range, except at wavelengths lower than 510 nm. This absorption effect is most likely to be associated with the presence of suspended organic matter and dissolved organic matter adsorbed to the suspended particles (Dekker, 1993; Kirk, 1994).

Lake Aritapera is located in the interior of an island in the Amazon River. The fractional abundance of suspended inorganic matter determined for this lake was 0.55 during high water and 1.01 during falling water. This result shows agreement with the physical characteristics of this lake and the spectral variation observed from the images; evidencing conditions of high SIM concentration during the falling water period. Suspended inorganic matter concentration becomes higher over shallow regions of the floodplain lakes as the water level falls. The gradual increase of SIM concentration causes reflectance elevation over the VIS and IVP spectral range. However, at a certain point of transition from high SIM concentrations to muddy water, the increase upon the reflectance stops occurring as much over the VIS and begins to occur more intensively over the IVP. As this gradually occurs, the spectral response becomes similar to a soil spectrum. This effect on the reflectance at high concentrations of SIM brings severe complications to the spectral mixture analysis, once the scattering produced in the IVP range is also a characteristic of phytoplankton cells. Hence, the increase in $f_{phytoplankton}$ mapped for this lake during the falling period is uncertain (**Figure 4**). As mentioned before the RMS error image presented greater uncertainties in shallow water lakes.

The Hyperion images showed important spectral variability between high and falling water periods over Lake Curumu. During high water, a situation of non turbid ground water with high loads of DOM mixing with SIM coming from the Amazon River was observed, and the LSU calculated 0.31 for f_{SIM} and negative values for $f_{phytoplankton}$. A phytoplankton bloom was observed at the moment of the acquisition of the falling water Hyperion image, and the LSU calculated 0.12 for f_{SIM} and 0.51 for $f_{phytoplankton}$ (**Figure 4**)**.** According to the physical characteristics of this lake, the concentration of SIM is actually expected to increase towards falling water, instead of decreasing as indicated by comparing the values of f_{SIM} determined for the two periods. This can be explained by the fact that at falling water the phytoplankton bloom occurred close to the surface, while SIM distributed itself more homogeneously along the water column.

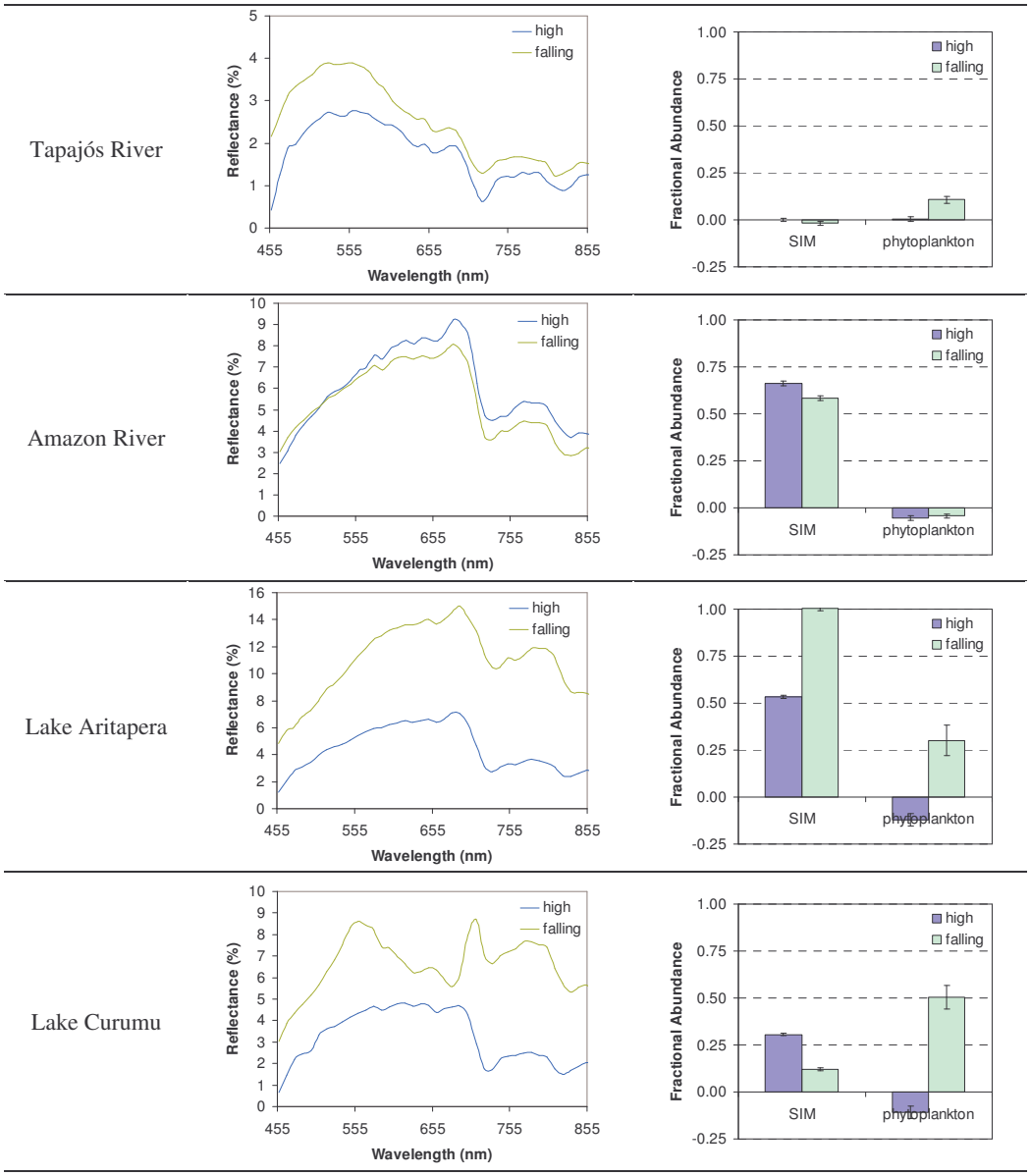

Figure 4 - Temporal variability of reflectance and SIM and phytoplankton end-member abundances calculated for water bodies selected over the floodplain.

7. Conclusion

The temporal dynamics in water composition changes in the floodplain are intense along the seasons. Hence, the approach of "key" spectral end-member selection from Hyperion data from both periods included in the analysis (high and falling water), favored for a greater availability of pure pixels dominated by each individual OAS. The authors recommend that future studies should continue to consider hyperspectral images to characterize the spectral mixtures in the Amazon floodplain multicomponental waters, seeking for a better understanding of the spatial-temporal dynamics.

Three distinct general tendencies of water composition variation from high to falling flood periods were observed from the results of Linear Spectral Unmixing of two temporal Hyperion images, acquired over the Central Amazon Floodplain region: increase of SIM and phytoplankton concentrations, in *varzea* lakes; increase of phytoplankton concentration, in the Tapajós River; and decrease of SIM concentration in the Amazon River.

Acknowledgments

Conrado M. Rudorff thanks CAPES for offering scholarship funds during two years of Remote Sensing Master Course at INPE, where the research that originated this article took place. The authors thank NASA/LBA-Ecology for image acquisition and financial support. The authors also thank GEOMA-MCT program for partial support of this research.

References

Adams, J. B.; Smith, M. O.; Johnson, P. E. Spectral mixture modeling: A new analysis of rock and soil types at the Viking Lander 1 site. **Journal of Geophysical Research**, v. 91, p. 8098-8112, 1986.

AIG. **ACORN User's Guide, Stand Alone Version.** Boulder, CO: Analytical Imaging and Geophysics LLC, 2001.

Aspinall, R. J.; Marcus, W. A.; Boardman, J. W. Considerations in collecting, processing, and analysing high spatial resolution hyperspectral data for environmental investigations. **Journal of Geographical Systems**, v. 4, n.1, p. 15-29, 2002.

Barbosa, C. C. F. **Sensoriamento Remoto da dinâmica de circulação da água do sistema planície de Curai / rio Amazonas.** 2005. 281 p. Tese (Doutorado em Sensoriamento Remoto) - Instituto Nacional de Pesquisas Espaciais, São José dos Campos. 2005.

Bukata, R. P. J., J.H.; Kondratyev, K.Ya.; Pozdnyakov, D.V. **Optical Properties and remote Sensing of Inland and Coastal Waters.** Boca Taton, Florida: CRC Press LLC, 2000. 362 p.

Dekker, A. G. **Detection of Optical Water Quality Parameters for Eutrophic Waters by High Resolution Remote Sensing.** 1993. 222 p. (Doctoral) - University of Amsterdam, Amsterdam. 1993.

Green, A. A.; Berman, M.; Switzer, B.; Craig, M. D. A transformation for ordering multispectral data in terms of image quality with implications for noise removal. **IEEE Transactions on Geoscience and Remote Sensing**, v. 26, n.1, p. 65 - 74, 1988.

Han, T.; Goodenough, D. G.; Dyk, A.; Love, J. Detection and correction of abnormal pixels in Hyperion images. In: IEEE Geoscience and Remote Sensing Symposium (IGARSS). 2002, Toronto, ON, Canada. **Proceedings…** IEEE International, 2002. Artigos, p. 1327-1330. On-line. ISBN 0-7803-7536-X. Disponível em: <http://ieeexplore.ieee.org/xpls/abs_all.jsp?isnumber=22038&arnumber=1026105&count=211&index=8>. Acesso em: October 21, 2005.

Junk, W. J. **The central Amazon floodplain.** Berlin: Springer, 1997. 525 p.

Kirk, J. T. O. **Light and photosynthesis in aquatic ecosystems. .** Cambridge: Cambridge University Press, 1994.

Kruse, F. A.; Boardman, J. W.; Huntington, J. F. Comparison of airborne hyperspectral data and EO-1 Hyperion for mineral mapping. **IEEE Transactions on Geoscience and Remote Sensing**, v. 41, n.6, p. 1388-1400, 2003.

Kruse, F. A.; Lefkoff, A. B.; Boardman, J. W.; Heidebrecht, K. B.; Shapiro, A. T.; Barloon, P. J.; A.F.H., G. The spectral Image-Processing System (Sips) - interactive visualization and analysis of imaging spectrometer data. **Remote Sensing of Environment**, v. 44, n.2-3, p. 145-163, 1993.

Mertes, L. A. K.; Smith, M. O.; Adams, J. B. Estimating suspended sediment concentrations in surface waters of the Amazon River wetlands from Landsat images. **Remote Sensing of Environment**, v. 43, n.3, p. 281-301, 1993.

Novo, E. M. L. M.; Shimabukuro, Y. E. Spectral Mixture Analysis of Inland Tropical Waters. **International Journal of Remote Sensing**, v. 15, n.6, p. 1351-1356, 1994.

Novo, E. M. L. M.; Steffen, C. A.; Braga, C. Z. F. Results of a laboratory experiment relating spectral reflectance to total suspended solids. **Remote Sensing of Environment**, v. 36, n.1, p. 67-72, 1991.

Rudorff, C. M.; Novo, E. M. L. M.; Galvão, L. S. Spectral mixture analysis of inland tropical Amazon Floodplain waters using EO-1 Hyperion. In: IEEE Geoscience and Remote Sensing Symposium (IGARSS). 2006, Denver, USA. **Proceedings...** IEEE International, 2006. Artigos. CD-ROM.